



Original article

On “Generalized Upper Bound” method and its application to some plane strain compression and extrusion problems

Nitai S. Das^a, Hillol Joardar^a, Matruprasad Rout^b, Bikash C. Behera^a, *Kalipada Maity^c

^aDepartment of Mechanical Engineering, C. V. Raman Global University, Bhubaneswar, India

^bDepartment of Mechanical Engineering, National Institute of Technology Tiruchirappalli, Trichy, India

^cDepartment of Mechanical Engineering, National Institute of Technology Rourkela, Odisha, India

ABSTRACT

This paper outlines the salient features of the “generalized upper bound” technique and uses it to derive upper bounds for plane strain compression and extrusion of metals in the presence of Coulomb friction ($\tau = \mu p$). For compression the velocity field is established by reformulating the same proposed earlier by Lee and Altan so as to be compatible with the interface Coulomb friction condition. For extrusion, the upper bound velocity field is derived from a stream function for flow through a smooth die of wedge angle $(\alpha + \lambda)$ where, α is the semi-wedge angle of the rough die, and λ is the friction angle ($\tan \lambda = \mu$). Analysis for this case is also presented assuming the flow to be radial. The analytical results are compared with those obtained from, the slip-line field and finite element analyses and from the rigid triangle velocity fields. These are also validated by some experimental results available in literature.

Key words: Coulomb friction; Upper bound; Plain strain; stream function compression; extrusion; Finite element modelling

1. INTRODUCTION

For most metal working operations, exact analytical solutions are difficult to obtain. Hence, approximate methods, based on limit analyses are used to get an estimate of the forming load.

The most widely used of these methods is the upper bound method since, it provides an overestimate on the actual load and ensures that the operation can be successfully completed.

The upper bound theorem may be stated as “for a plastically deforming medium, if a velocity field could be found that satisfies the continuity condition and the velocity boundary conditions, then the load calculated from such a velocity field is always higher than the actual load”. In particular, this field should be compatible with the rigid motion of the tool or die. A velocity field satisfying the above conditions is generally referred to as a kinematically admissible velocity field. Mathematically, the upper bound theorem may be stated as “among all the kinematically admissible strain rate fields, the actual one minimizes

the expression (Prager and Hodge [1], Drucker et al., [2]):

$$J^* = \frac{2}{\sqrt{3}} \sigma_0 \int_V \sqrt{v_2 \varepsilon_{ij} \varepsilon_{ij}} dv + \frac{\sigma_0}{\sqrt{3}} \int_{S_f} |\Delta v| ds - \int_{S_T} T_i V_i ds \quad (1)$$

In Eq. 1 the first term on the right represents the internal power of deformation over the volume V of the deforming medium. The second term includes the shear power over surfaces of velocity discontinuity including those between the tool and the deforming material. The third term covers the power due to the traction applied on the surface ST . For applying the upper bound inequality, the major problem lies in selecting a velocity field that satisfies the above-mentioned conditions. A number of techniques have been employed to tackle this problem. Thus, for plane strain and axisymmetric operations, one such approach

* Corresponding author's e-mail: kalipadamaity84@gmail.com

is to divide the deformation zone into rigid triangular elements and to assume the energy to be dissipated due to velocity discontinuities at the adjacent sides of the adjoining triangles [3-7]. Velocity fields have also been constructed by expressing these as continuous functions of the coordinates of a point within the deformation zone [8-10]. Alternatively, these may be derived from assumed stream functions [11, 12] or with the help of the conformal mapping technique [13, 14]. Velocity fields have also been established from assumed shape of the deformation zone boundaries [15-18]. Quite a large number of problems have been solved using the above techniques and an excellent account of these analyses may be found in the books by Johnson and Mellor [19] and Avitzur [20].

When the energy dissipation rate J^* (equation 1) due to such a velocity field is equated with the external rate of work by the die or the tool, an upper bound on the deformation load is obtained.

For problems where the die/metal interface friction is expressed by the shear friction law, $\tau = mk$, the friction work can be calculated in a straight forward manner and an upper bound on the forming load may be readily obtained with the help of equation (1). When the interface friction is governed by Coulomb's law ($\tau = \mu p$) however, estimation of the friction work and hence the upper bound is not so simple as the friction stress in this case is a function of the local die pressure which is unknown. None-the-less, some knowledge of the forming load for these problems may be obtained using the methods suggested by Drucker [21], Kudo [6,7], Solhjo [22] or with the help of the slab method of analysis [23].

For plane strain problems and where the deformation zone is discretized into rigid triangular elements, upper bounds on forming load, under coulomb friction condition, may be obtained by considering the equilibrium of normal and tangential forces on the sides of each element (momentum approach). Westwood and Wallace [24] used this method to calculate the loads for tube drawing, rod drawing/extrusion and compression. The same was also used by Green and Wallace [25], Green, Sparling and Wallace [26] for flat rolling. When the deformation zone involves a single triangle as in the case metal machining [27] or in the case of extrusion through a short wedge-shaped die [28, 29], calculation of the upper bound using the above method is quite simple. As the number of triangular elements increase however, the equations originating using this method become complex and the "energy approach" appears to provide a better choice.

In 1969 [30], Collins formulated the "Generalized Upper Bound Method" which could be used to construct admissible velocity fields, when the die/metal interface friction is governed by Coulomb's law. He argued that the upper bound inequality stated by the equation

$$\int_{S_u} T_i u_i^* ds_u \leq \int_v \sigma_{ij}^* ds_f \quad (2)$$

Holds irrespective of whether u^* is incompatible with the actual velocity conditions on S_u . In other words, u^* need not be kinematically admissible. The only requirement for

u^* is that it should be constant, so that it can be taken outside the integral sign. Hence, for applying the upper bound technique, the trial velocity field should be selected on the consideration that it provides an upper bound on the "quantity of interest", rather than whether it satisfies the actual velocity boundary conditions on the tool or die. He further stated that if the trial velocity field is such that its component in the direction of the resultant surface traction is constant, then such a velocity field would provide an upper bound on the forming load for the coulomb friction condition. Collins [30] applied this method for the calculation of the upper bounds on load for strip compression and extrusion and found reasonable agreement with the corresponding slip-line field solutions. For the above calculations, he used velocity fields that were composed of rigid triangular elements separated by straight lines of velocity discontinuity.

Yu and Sloan [31] developed a finite element model based on the above upper bound approach and applied it for the determination of the bearing capacity of footings, resting on a cohesive soil. In spite of its importance in the analysis of the metal forming processes, however, its application to such problems, till date, has remained limited only to the two examples discussed by Collins in his original paper.

In this investigation, new upper bound solutions for some plane strain metal forming operations are presented using the above method. The forming problems considered are the plane strain compression of a strip by two parallel overhanging platens and the plane strain extrusion through a wedge-shaped die using a flat rigid punch. Coulomb friction is assumed and the material is taken to be rigid-perfectly plastic. For compression, the velocity field is derived by modifying the same proposed earlier by Lee and Altan [32] and accounts for mid-plane bulging. For extrusion, the velocity field is constructed using a stream function [11] for flow through a smooth die of semi wedge-angle $(\alpha + \lambda)$, where α is the semi wedge-angle of the rough die and λ is the friction angle ($\tan \lambda = \mu$). Solutions for this case are also obtained assuming the flow to be radial [9]. Approximate upper bounds for both cases are computed considering the pressure to be uniformly distributed at the die/metal interface. The analytical results are validated by those obtained using the slip-line field analysis and the finite element technique. These are also compared with some experimental results available in literature.

2. UPPER BOUND ANALYSIS

2.1 STRIP COMPRESSION WITH BULGING

We consider the plane strain compression of a strip of initial width $2D$ and initial thickness $2H$ by two opposed overhanging platens moving with the same velocity in opposite directions as shown in Fig. 1. The presence of interface friction restrains the relative motion between the layers of material, resulting in free surface barreling or bulging. Due to the presence of barreling, the strip width becomes maximum at the mid-plane and minimum at the die/metal interface.

Lee and Altan [32] have presented a kinematically admissible velocity field for this case. This may be written as,

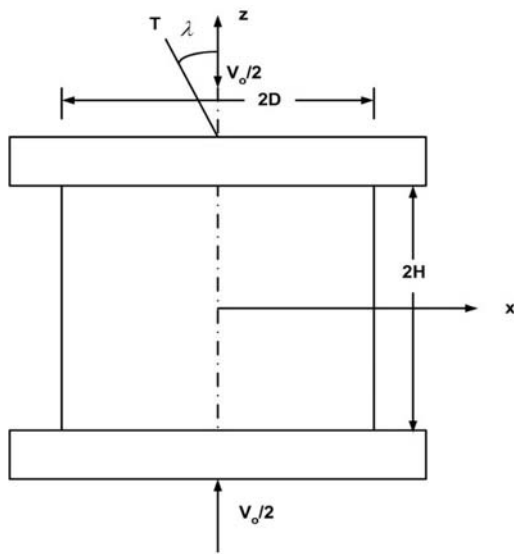
$$u_x = Ax(1 - \beta z^2) \quad (3a)$$

$$u_z = -Az(1 - \beta z^2)/3 \quad (3b)$$

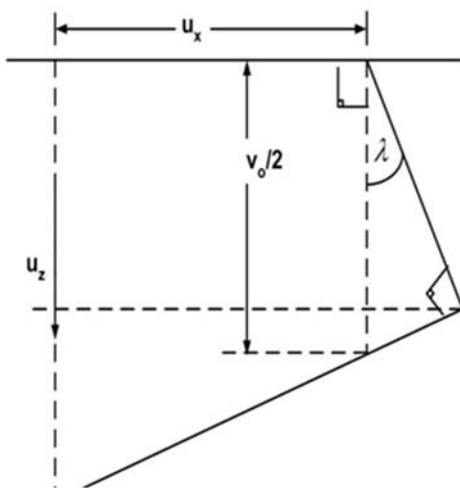
And

$$u_y = 0 \quad (3c)$$

where, x, y and z are the coordinates of a point within the deformation zone, β is the barreling parameter and A is a constant (Figure 1a)



(a)



(b)

Fig. 1 Plane strain compression of a strip by overhanging platens (a) Physical plane and (b) Hodograph

For Coulomb friction condition, the material velocity at the die/metal interface must lie on the line normal to the

direction of the resultant surface traction [30]. Hence, the above velocity field is modified to (Fig. 1b)

$$u_x = Ax(1 - \beta z^2) \quad (4a)$$

$$u_z = -Az((1 - \beta z^2)/3 - \mu Ax(1 - \beta z^2)f(z)) \quad (4b)$$

And

$$u_y = 0 \quad (4c)$$

Where, $f(z)$ is a function of z and should be such that,

$$f(z) = 0 \text{ at } z = 0 \text{ and } f(z) = 1 \text{ at } z = H$$

at $z = H$ and $x = 0$,

$$u_z = v_0/2H = \text{downward velocity of the top platen.}$$

Hence,

$$A = \frac{v_0}{2H} (1 - \beta H^2/3) \quad (5)$$

Referring to Eq. 4, it may be seen that it satisfies the necessary velocity boundary conditions:

$$u_x = 0 \text{ at } x = 0$$

$$u_x = \text{maximum at } x = D$$

$$u_z = 0 \text{ at } z = 0$$

$$u_z = -v_0/2 \text{ at } z = H \text{ and } dx = 0$$

Also, on the die face,

$$u_z + \mu u_x = v_0/2 = \text{Constant} \quad (6)$$

The above equation satisfies the boundary conditions on velocity as stated by Collins [30].

The strain rate ϵ components may be derived using Eq. 4. These are written as,

$$\epsilon_x = A(1 - \beta z^2) \quad (7a)$$

$$\epsilon_z = -A(1 - \beta z^2) - \mu Ax(-2\beta z f(z) + (1 - \beta z^2)f'(z)) \quad (7b)$$

$$\gamma_{yz} = \frac{1}{2}(-2A\beta xz - \mu Ax((1 - \beta z^2)f(z))) \quad (7c)$$

$$\epsilon_y = \gamma_{xy} = \gamma_{yz} = 0 \quad (7d)$$

The compression load for the strip is given by

$$P/2K = 4W_i$$

Where,

$$W_i = \int_0^D \int_0^H (\frac{1}{2}(\epsilon_x^2 + \epsilon_z^2) + \gamma_{xz}^2)^{1/2} dx dz \quad (8)$$

And the average pressure is written as

$$\bar{p}/2k = \frac{2W_i}{D} \quad (9)$$

where, k is the yield stress in shear of the work material

Equation (8) after substitution of Eq.(7) was integrated by 8-point Gaussian quadrature to determine the mean die pressure for different width to thickness ratios(D/H) and

for different values of μ . For the purpose of the above integration, $f(z)$ was assumed to be either,

$$f(z) = z/H \quad (10a)$$

or

$$f(z) = \sin\left(\frac{\pi}{2} \cdot \frac{z}{H}\right) \quad (10b)$$

It may be seen that the velocity boundary conditions are also satisfied if u_z is expressed as:

$$u_z = -Az(1 - \beta z^2/3) - \tan\left(\frac{\lambda}{H}z\right)Ax(1 - \beta z^2) \quad (11a)$$

or

$$u_z = -Az(1 - \beta z^2/3) - \mu Ax(1 - \beta z^2)z^{(H-z)} \quad (11b)$$

The plastic work rate for the same cases were computed using the same procedure as that outlined above.

An alternative expression for \bar{p} , for this case may be obtained in the following manner. The total energy dissipation rate in compression may be written as

$$J^* = \dot{W}_d + \dot{W}_f \quad (12)$$

Where, W_d is the deformation power, when $\mu = 0$ and W_f is the friction power. W_d can be calculated from Eq. (8) by substituting $\mu = 0$. We assume the normal pressure to be uniformly distributed over the die face. Hence, friction power is given by,

$$\dot{W}_f = \mu PA(1 - \beta H^2)D \quad (13)$$

where, P is the die load. Hence,

$$\bar{p}/2k = 2\dot{W}_d/(1 - \mu A(1 - \beta H^2)D)D \quad (14)$$

2.2 STRIP EXTRUSION

The extrusion of a rigid-perfectly plastic strip of initial thickness $2H$ to a final thickness $2h$ through a straight wedge-shaped die of semi-wedge angle α is demonstrated in Fig. 2, only the upper half of the deformation zone being indicated for reason of symmetry. The upper bound deformation mode for this problem, proposed by Collins [30], consisting of a single rigid triangle is shown in Fig. 2a. In the hodograph diagram (Fig. 2b), line 'bd' represents the velocity in the direction of the resultant surface traction T . Line cd is normal to line bd . It may be seen that line cd extended meets the horizontal at an angle of $(\alpha + \lambda)$ where, $\tan \lambda = \mu$. Thus, for upper bound calculation, for extrusion through rough a die of semi wedge-angle α , the velocity field should be that for a smooth die of semi wedge-angle $(\alpha + \lambda)$. This concept is used to define a stream function for this problem as discussed below:

Let AB represent the die of semi-wedge angle α , and AC the die of semi-wedge angle $(\alpha + \lambda)$, as shown in Fig.3. H_c is the billet thickness at entry to the die AC . Then,

$$H_c = h + L \tan(\alpha + \lambda) \quad (15a)$$

$$H = h + L \tan \alpha \quad (15b)$$

where, L is the die length.

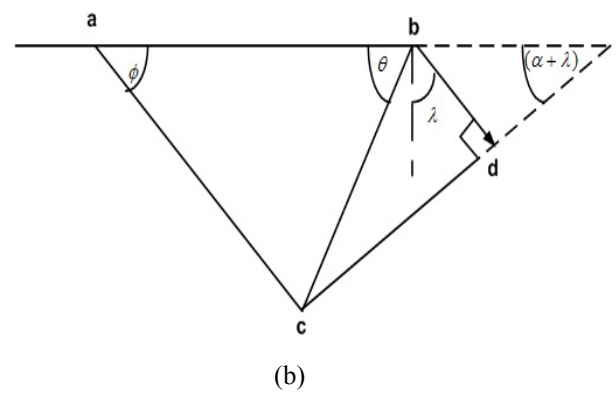
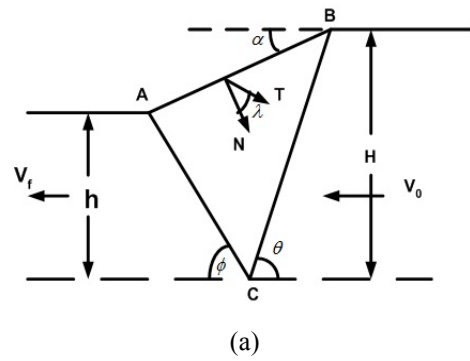


Fig. 2 Collins upper bound velocity field (a) Physical plane and (b) Hodograph

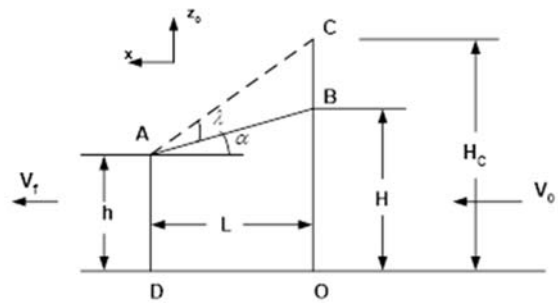


Fig. 3 Die configuration for present analysis. AB is the rough die of semi-wedge angle α . AC is the smooth die with semi-wedge angle $(\alpha + \lambda)$.

Following Nagpal [11], the stream function for the plane strain flow through a die of semi-wedge angle $(\alpha + \lambda)$ in the given coordinate system may be written as,

$$\Psi = H_c V_0 z_c / (H_c - x \tan(\alpha + \lambda)) \quad (16)$$

Where, x and z_c are the coordinates of a point in the deformation zone $OACD$ and V_0 is the billet velocity at die entry.

The velocity components can now be calculated with the help of the following equations. Thus,

$$u_x = \frac{d\psi}{dz} = H_c V_0 / (H_c - x \tan(\alpha + \lambda)) \quad (17a)$$

$$v_z = -\partial\Psi/\partial x = -H_c V_0 \tan(\alpha + \lambda) z_c / (H_c - x \tan(\alpha + \lambda))^2 \quad (17b)$$

and the strain rate components are given by,

$$\epsilon_x = H_c V_0 \tan(\alpha + \lambda) / (H_c - x \tan(\alpha + \lambda))^2 \quad (18a)$$

$$\epsilon_z = -H_c V_0 \tan(\alpha + \lambda) / (H_c - x \tan(\alpha + \lambda))^2 \quad (18b)$$

and

$$\gamma_{xz} = H_c V_0 \tan^2(\alpha + \lambda) z_c / (H_c - x \tan(\alpha + \lambda))^3 \quad (18c)$$

$$\epsilon_y = \gamma_{xy} = \gamma_{yz} \quad (18d)$$

The effective strain rate at any point within OCAD is given by,

$$\dot{\epsilon} = \sqrt{(1/2)(\epsilon_{ij} \cdot \epsilon_{ij})} = \sqrt{\frac{1}{2}(\epsilon_x^2 + \epsilon_z^2) + \gamma_{xz}^2}$$

Hence,

$$\bar{\epsilon} = \frac{H_c V_0 \tan(\alpha + \lambda)}{(H_c - x \tan(\alpha + \lambda))^2} \left(1 + \frac{\tan^2(\alpha + \lambda) z_c^2}{(H_c - x \tan(\alpha + \lambda))^2}\right)^{1/2} \quad (19)$$

Eqn. (19) provides the effective strain rate at a point within OABD with co-ordinate (x z).

Where z is defined by (mapping points in OCAD to those in OABD)

$$z = \frac{z_c(h-x \tan \alpha)}{(h_c-x \tan(\alpha+\lambda))} \quad (20)$$

The deformation work W_i within OABD is given by:

$$W_i = \frac{2\sigma_0}{\sqrt{3}} \int_0^L \int_0^H \frac{H-x \tan \alpha}{H_c V_0 \tan(\alpha+\lambda)^2} \left(1 + \frac{\tan^2(\alpha+\lambda) z_c^2}{(H_c-x \tan(\alpha+\lambda))^2}\right)^{1/2} dz dx \quad (21)$$

where, σ_0 is the yield stress in compression of the work material. Eqn.(21) after substitution of eqn.(20) can be integrated using any standard quadrature formula or by the method of Finite difference. In the present case W_i was calculated using 8-point Gaussian quadrature. For the above calculation V_0 was taken equal to unity.

Nagpal [11] has shown that the surfaces of velocity discontinuity at entry and exit for the assumed stream function (Eq. 16) will be vertical as shown in Fig 3. The work rate due to velocity discontinuity at entry plane OB is written as:

$$W_{en} = k \cdot \frac{H_c \tan(\alpha+\lambda)}{H_c^2} \cdot \frac{H_c}{H} \int_0^H z dz = \frac{kH \tan(\alpha+\lambda)}{2} \quad (22a)$$

$$W_{ex} = K \cdot \frac{H_c \tan(\alpha+\lambda)}{H_c^2} \cdot \int_0^H z dz = \frac{kH_c \tan(\alpha+\lambda)}{2} \quad (22b)$$

The mean extrusion pressure is therefore, evaluated using the equation

$$\bar{P}/2k = (W_i + W_k + W_{ex})/2kH \quad (23)$$

where, $K = \frac{\sigma_0}{\sqrt{3}}$ is the yield stress in shear of the work material.

An approximate expression for the mean extrusion pressure for this case is also obtained if the normal pressure is assumed to be uniformly distributed over the die face. The total power J^* is written as,

$$J^* = W_d + W_f \quad (24)$$

Where, $W_d = W_i + W_{en} + W_{ex}$ is the total power of deformation, when $\mu = 0$ and W_f is friction power. W_d is evaluated from Eqs.21 and 22 by substituting $\lambda=0$. The friction work W_f is calculated in the following manner:

The material velocity parallel to the die face at any point in the die/metal interface is given by,

$$V_d = V_x / \cos \alpha = V_0 H / (H - x \tan \alpha) \cos \alpha \quad (25)$$

Hence, the friction work W_f is calculated using the equation,

$$W_f = \int dW_f = \mu \frac{N}{L} \int_0^L \frac{V_0 H dx}{(H - x \tan \alpha) \cos \alpha}$$

or

$$W_f = \mu V_0 N H \ln(H/h) / (H - h) \quad (26)$$

Where, N is the total normal load on the die surface given by,

$$N = P / (\sin \alpha + \mu \cos \alpha) \quad (27)$$

and L is the die length. Substituting equation (27) in equation (26), we have,

$$\bar{P}/2k = W_d / (1 - Q)H \quad (28)$$

where,

$$Q = \mu H \ln(H/h) / (H - h)(\sin \alpha + \mu \cos \alpha) \quad (29)$$

2.3 ANALYSIS FOR A RADIAL FLOW FIELD (PLANE STRAIN EXTRUSION)

For upper bound analysis of axis symmetric extrusion/drawing through a conical die, Avitzur [9] assumed the deformation region to be part of a sphere with the flow taking place in the radial direction. Such a velocity field is referred to as a spherical velocity field or a radial flow field. For plane strain extrusion through a similar die, the deformation region is taken to be part of a cylinder.

Fig. 4(a) shows the upper half of the deformation zone for the radial flow field where AB is the die with semi-wedge angle “ α ” and AC, the die with semi-wedge angle ($\alpha+\lambda$). AB has its apex at P and AC at the origin ‘O’ of the coordinate system. Circular arcs CBD and AIJ with their centre at ‘O’ define the entry and the exit boundaries of the deformation zone respectively. The actual flow takes place through the die AB for which upper bound on the extrusion load is sought. H_c, H, h, V_0 and V_f in Fig 4 have the same meaning as those given in Fig.3, section 2.2.

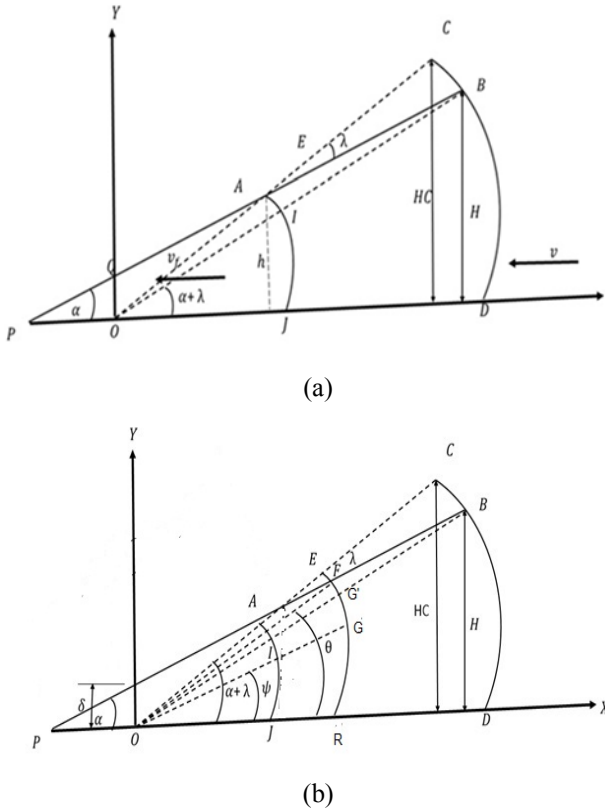


Fig. 4 Radial flow field

Referring to Fig.4-a, it may be seen that

$$OA = \frac{h}{\sin(\alpha+\lambda)} \quad (30a)$$

$$PA = \frac{h}{\sin \alpha} \quad (30b)$$

$$OC = OB = ((OA \cos(\alpha + \lambda) + AB \cos \alpha)^2 + H^2)^{1/2} \quad (30c)$$

$$H_c = OC \sin(\alpha + \lambda) \quad (30d)$$

$$AB = \frac{(H-h)}{\sin \alpha} \quad (30e)$$

$$AC = \frac{(H_c-h)}{\sin(\alpha+\lambda)} \quad (30f)$$

$$V_f = H_c \frac{V_o}{h} \quad (30g)$$

Let EFR be a circular arc of radius r that intersects AB at F (Fig.4b). The coordinates X_F and Y_F of point F can be calculated in the following manner:

$$X_F^2 + Y_F^2 = r^2 \quad (31a)$$

$$Y_F = X_F \tan \alpha + OQ \quad (31b)$$

$$OP = \left(\frac{h}{\tan \alpha} \right) - \left(\frac{h}{\tan(\alpha+\lambda)} \right) \quad (31c)$$

$$OQ = h \left(1 - \frac{\tan \alpha}{\tan(\alpha+\lambda)} \right) \quad (31d)$$

Eliminating Y_F from equation (31a) and (31b), a quadratic in X_F is obtained. This is written as,

$$X_F \sec^2 \alpha + 2OQ X_F \tan \alpha + OQ^2 = r^2 \quad (32)$$

Retaining only the positive root, X_F is finally given by

$$X_F = ((r^2 \sec^2 \alpha - OQ^2)^{1/2} - OQ \tan \alpha) \cos^2 \alpha \quad (33a)$$

Hence,

$$Y_F = ((r^2 \sec^2 \alpha - OQ^2)^{1/2} - OQ \tan \alpha) \sin \alpha \cos \alpha + OQ \quad (33b)$$

and,

$$\theta_F = \arctan \frac{Y_F}{X_F} \quad (33c)$$

To determine the strain at any point in the flow zone $ABDJ$, it is necessary to know its mapped location in the deformation region $ACDJ$. Let G be a point on the circular arc FGR in $ABDJ$ (Fig. 5(b)). It may be seen that its image G' in $ACDJ$ will lie on the circular arc EFR . Let (r, ψ) and (r, ψ_c) be the polar coordinates of G and G' respectively. Then ψ_c is given by:

$$\psi_c = \frac{(\alpha+\lambda)\psi}{\theta_F} \quad (34)$$

The velocities and strain rates at point G corresponding to those at point G' , may be calculated with the help of the following equations. Thus, the radial velocity

$$u_r = -OAV_f \cos\left(\frac{\psi_c}{r}\right) \quad (35)$$

Hence,

$$\varepsilon_r = \frac{\partial u_r}{\partial r} = OAV_f \cos \psi_c / r^2 \quad (36a)$$

$$\varepsilon_\theta = \frac{u_r}{r} = -OAV_f \cos \psi_c / r^2 \quad (36b)$$

And,

$$\gamma_{r\theta} = \frac{1}{2} \frac{\partial u_r}{r \partial \theta} = \frac{OA}{2r} V_f \sin \psi_c / r \quad (36c)$$

All other strain rate components are zero. The rate of internal energy dissipation is given by

$$W_i = \frac{2}{\sqrt{3}} \sqrt{\frac{\varepsilon_{ij} \varepsilon_{ij}}{\sqrt{3}}} = \frac{2\sigma_0}{\sqrt{3}} OAV_f \int_{JA} \int_{BD} \frac{1}{r^2} (\cos^2 \psi_c + \frac{\sin^2 \psi_c}{4})^{1/2} dr d\psi \quad (37)$$

The work done due to velocity discontinuities at entry and exit can now be calculated. The shear work W_{en} at entry is given by,

$$W_{en} = \int_0^{\theta_B} \frac{\sigma_0}{\sqrt{3}} OB d\psi V_o \sin \psi_c$$

or,

$$W_{en} = \frac{\sigma_0}{\sqrt{3}} OB V_o \frac{\theta_B}{(\alpha+\lambda)} (1 - \cos(\alpha + \lambda)) \quad (38)$$

Similarly, the shear work W_{ex} at exit is calculated using the equation,

$$W_{ex} = \int_0^{(\alpha+\lambda)} \frac{\sigma_0}{\sqrt{3}} OAV_f \sin \psi d\psi \quad (39)$$

It may be seen that when $\lambda=0$, $\theta_B=\alpha$ and $W_{en}=W_{ex}$. θ_B can be calculated from equation (33) by substituting $r=OB$. Hence, the total work of deformation J^* is given by,

$$J^* = W_i + W_{en} + W_{ex} \quad (40)$$

Can be calculated and p determined using the relation,

$$\frac{\bar{p}}{2K} = \frac{J^*}{2kH} \quad (41)$$

where,

$k = \sigma_0/\sqrt{3}$ is the shear stress at yield of the work material.

In the present investigation, J^* was computed by integrating numerically equation (37) by trapezoidal rule using a step size of 25 ($d\psi = \theta/25$, $dr = AB/25$)

3. FINITE ELEMENT MODELING

The finite element analysis was carried out using the DEFORM 2D (V10) simulation system designed to analyze two-dimensional flow in complex metal forming processes. The system makes use of Lagrangian incremental formulation for the simulation. For this analysis the platen (compression) and the die and the punch (extrusion) were considered rigid, while the billet was assumed to deform plastically according to the rigid-plastic constitutive equation,

$$\sigma_0 = 250\epsilon^{0.0} \text{ Mpa} \quad (42)$$

The stress-strain diagram corresponding to the above constitutive equation is shown in fig.5. For compression, the specimen height ‘H’ was maintained constant at 20 mm and its width ‘D’ was varied from 20mm to 60mm to determine the forging pressure at different width/thickness (D/H) ratios. The simulation used 912 four noded quadrilateral elements with 970 nodes.

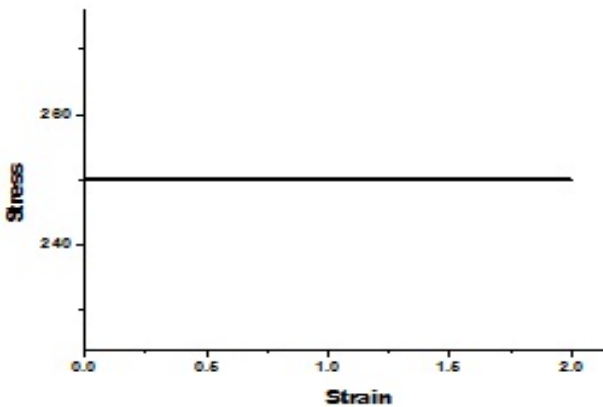


Fig. 5 The stress-strain diagram of the deforming material (Equation.42)

For extrusion, three different dies of semi-wedge angle $\alpha = 15, 30$ and 45 degrees were considered. The billet height, in this case was taken equal to 10mm and its initial length was 30mm. Two different meshing patterns were used in this analysis. For lower reductions, the mesh size was uniform throughout the deformation zone. The total number of elements in this case was 1000 with 1071 nodes. At higher reduction, finer mesh was used at die/metal contact region, and coarser mesh at rest of the areas. The total number of elements in this case was 1060 with 1123 nodes. Rectangular elements were used in all cases. Remeshing was adopted when the penetration of the mesh into the die at contact region exceeded 0.7mm.

Contact option in all cases was coulomb friction, with coefficient of friction $\mu=0.1, 0.2$ and 0.3 . All simulations were carried out assuming a constant work-piece temperature of 25°C . The punch movement was 1 mm/sec and temperature rise due to plastic deformation was neglected.

4. RESULTS AND DISCUSSION

The upper bound on compression pressure calculated using equation (9) was minimized with respect to the bulge parameter β with the help of a standard program based on the ‘Golden section’ minimization method [33]. The variation of this pressure with width to thickness ratio (D/H) is presented in Figure 6 as a function of the interface friction coefficient μ . The results indicated there are for $F(z)=z/H$ (Eqn.10(a)). Die pressures were also computed by defining $F(z)$ as given by equations 10(b) and 11(a) ($F(z) = \sin(\frac{\pi}{2} \cdot \frac{z}{H})$) or ($F(z) = \tan(\lambda z/H)$). However, over the solution range, the computed results for the three cases were found to differ by only 1%. The results from the finite element simulations are also seen to compare well with these upper bounds: the discrepancy between the two being less than 10% over the solution range. The bounds on forming load, calculated using equation (14) (uniform pressure distribution), were found to yield acceptable results only at low values of μ and at low width to thickness ratios. These were far in excess of the above upper bounds at higher values of μ and higher (D/H) ratios. Thus, for $\mu=0.1$ and $D/H=5$, the results from equation (14) exceeded those calculated from equation (9) by about 20%. But this difference increased to about 50% for $\mu=0.2$ and to about 90% for $\mu=0.3$. For still higher values, the results for $\bar{p}/2k$ become negative. This happens when

$$\mu A(1 - \beta H^2) > 1.$$

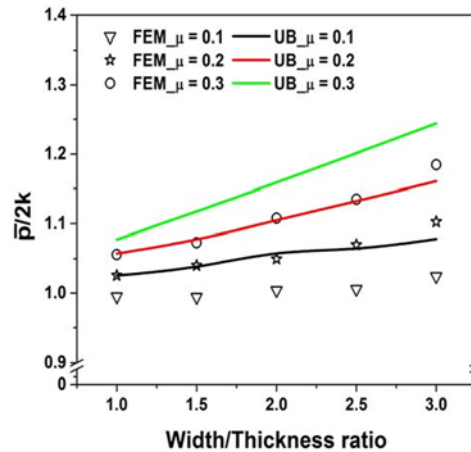


Fig. 6 Variation of mean die pressure with width/thickness ratio

The variation of forging load with platen travel in compression for a strip with $D=20\text{mm}$ and $H=30\text{mm}$ is depicted in Fig. 7, the corresponding increase in the contact and the equatorial widths being indicated in Fig. 8 and Fig.9 respectively. As expected, the load increases with increase in height strain. However, the effect of friction is found to be significant only at higher strain values. It may also be seen that in continued compression in plane strain, the increase in contact and equatorial widths are not sensitive to interface friction. This is found to be true both for upper bound and the finite element analyses. This is the agreement with the observation made by Fan [34].

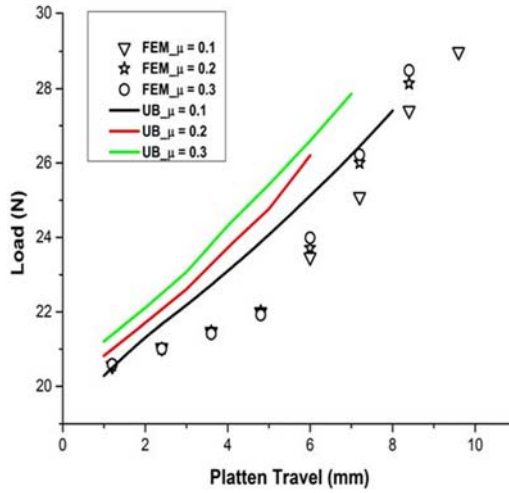


Fig. 7 Variation of load with decrease in specimen height

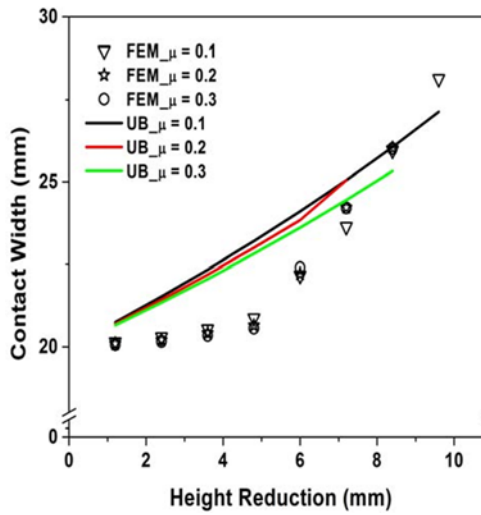


Fig. 8 Variation of contact width with reduction in height. Comparison of UBA with FEM

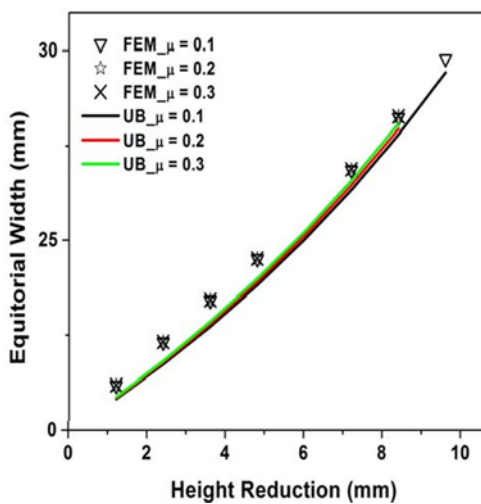
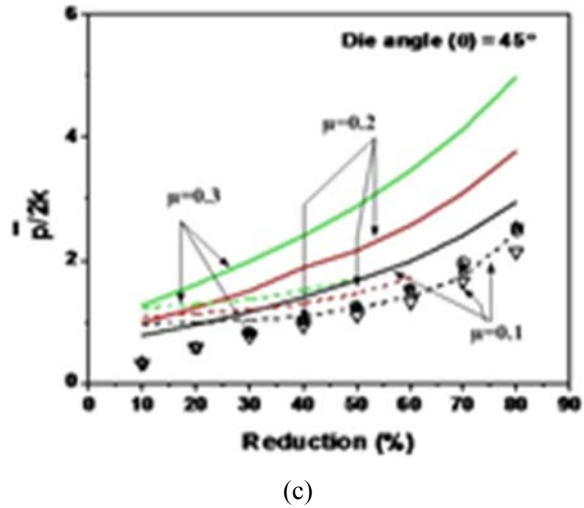
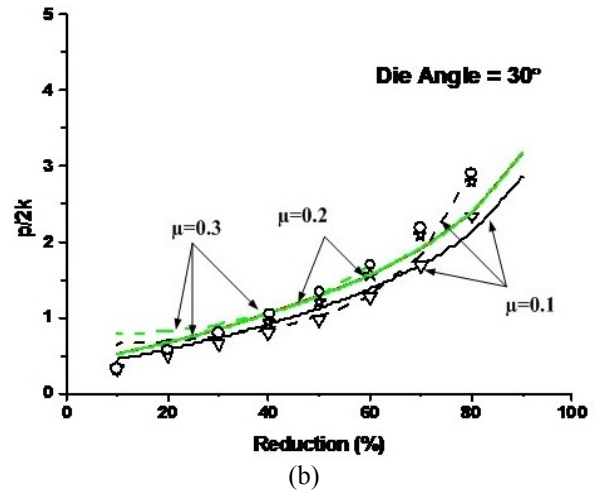
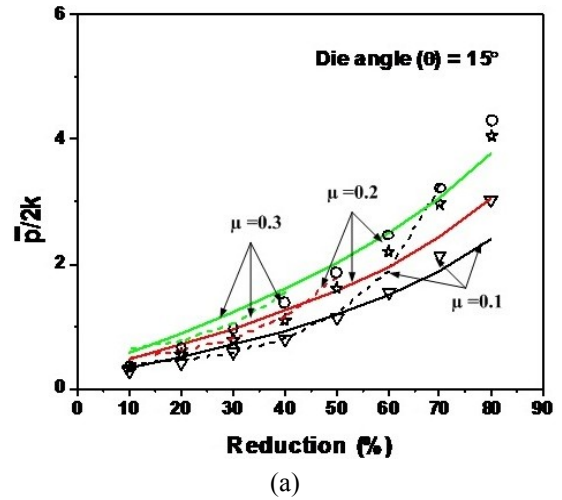


Fig. 9 Variation of equatorial width with reduction in height. Comparison of UBA with FEM



- (i) UB using present method (—)
- (ii) UB using rigid triangle velocity field (.....)
- (iii) Results using FEM ▽ μ=0.1, ★ μ=0.2, ○ μ=0.3

Fig.10 Variation of mean extrusion pressure with reduction for different die angles

The variation of mean extrusion pressure with reduction obtained from the present analyses are depicted in Figs 10

for die angles $\alpha = 15, 30$ and 45 degrees where these are compared with the same calculated from rigid triangle velocity fields [Collins,30] and from finite element simulation. The figures indicate that for $\alpha=15$ and 30 degrees, the present upper bounds are in general better than those derived by Collins [30] at lower (<20%) and higher (>50%) reductions. At intermediate reductions (20-50%), the results obtained from rigid triangle velocity fields are found to be superior (Figs.10-a and 10-b). For $\alpha=45$ degree however, the rigid triangle velocity field yields lower upper bounds at all reductions and friction conditions (Fig.10-c). These observations are seen to agree very well with the findings from the finite element simulation as well. An attempt was made to compare the above results with those obtained from the slip line field solutions [35-37]. But the results from the slip line field analysis did not differ from those obtained from the finite element analysis by more than 5%. Hence, these are omitted from the present figures for reason of clarity.

Calculations were also performed assuming the flow to be radial as described in section 3 (equation 40). However, for the same reduction and friction condition, these were found to be exactly equal to those obtained from equation (23), derived using a stream function. This is not surprising, since the stream lines satisfying the equation,

$$Z_c / (H_c - x \tan(\alpha + \lambda)) = Constant$$

Pass through the apex 'O' (Fig.4) indicating that the flow is radial. Mean pressures were also calculated assuming the pressure to be uniformly distributed over the die face (equation 28). But these were found to be acceptable only for low values of μ . This is in agreement with the observations mentioned earlier for compression.

Johnson [38] had carried out an extensive series of experiments for extrusion through square and wedge-shaped dies for comparison with his slip line field solutions. He presented his experimental results between two theoretical curves defining the two limiting conditions of friction, that is, $\mu=0$ and $\mu=\mu_{max}$.

Johnson's experimental results are compared within the present upper bounds in Figs 11-a and 11-b for $\alpha= 30$ and 45 degrees respectively. In these figures, the lower boundary refers to $\mu=0.1$ and the upper one to $\mu=0.3$. It may be seen that the experimental results agree reasonably well with the present upper bounds especially for $\alpha=30$ degrees (Fig.10-a).

However, for $\alpha= 45$ degrees, the experimental results seem to compare well with those calculated using rigid triangle velocity fields.

5. VELOCITY FIELDS FOR AXISYMETRIC OPERATIONS

For axis symmetric flow, the continuity equation may be written as,

$$\frac{\delta u_r}{\delta r} + \frac{u_r}{r} + \frac{\delta u_z}{\delta z} = 0 \tag{43}$$

With

$$\epsilon_r = \epsilon_\theta = -\frac{\epsilon_z}{2} \tag{44}$$

Hence, for axis symmetric compression the velocity field is written as,

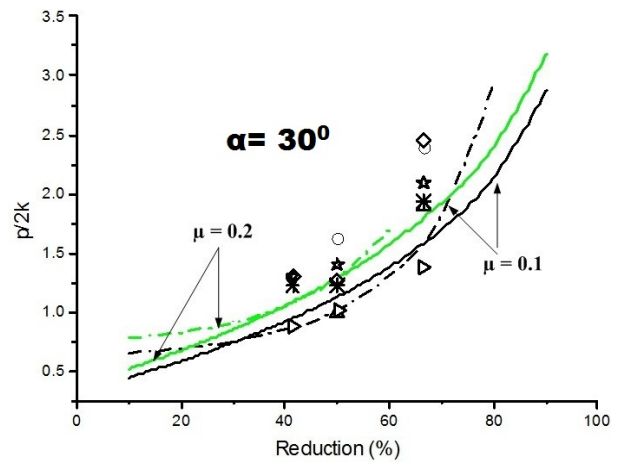
$$u_r = Ar(1 - \beta z^2) \tag{45}$$

$$u_z = -2Az \left(1 - \frac{\beta z^2}{3}\right) - \mu Ar(1 - \beta z^2)F(z) \tag{46a}$$

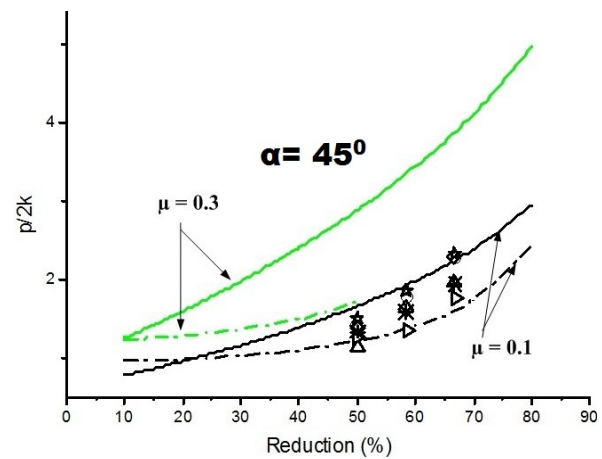
and,

$$u_\theta = 0 \tag{46b}$$

Where u_r , u_z and u_θ are the velocities in r , θ and z directions respectively (Fig 12). $F(z)$ in the above equation may be defined as in equation (10) or (11).



(a)



(b)

- (i) Present paper upper bound (—)
- (ii) Upper bound from rigid triangle velocity field (- -)
- (iii) Experimental results \bullet Pure lead unlubricated, \blacktriangle Pure lead lubricated, \blacklozenge Tellurium lead unlubricated, \blacktriangledown Tellurium lead lubricated, \blackstar Pure aluminium unlubricated, \blackstar Pure aluminium lubricated.

Fig.11 Comparison of present upper bounds with experimental

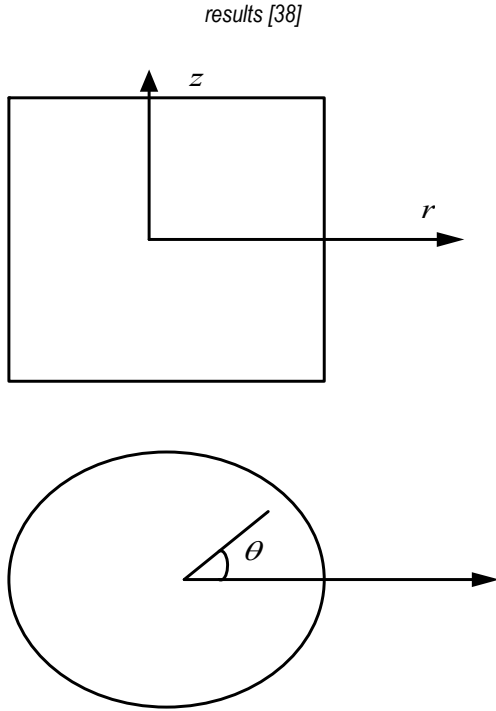


Fig. 12 Axisymmetric compression of a cylindrical billet

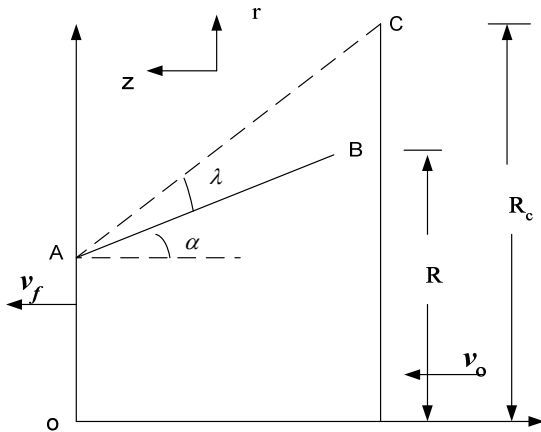


Fig. 13 Axisymmetric flow through a wedge shaped die

The stream function for axis symmetric extrusion is written as (Fig.13)

$$\psi = \frac{Cr_c^2}{2DF^2(z)} \quad (47)$$

where DF (Z) is the die profile function given by

$$DF(z) = R_c - z \tan(\alpha + \lambda) \quad (48)$$

The velocity components are given by,

$$u_z = \frac{1}{r_c} \frac{d\psi}{dr_c} = \frac{2c}{DF^2(z)} \quad (49a)$$

$$u_r = \frac{1}{r_c} \frac{d\psi}{dz} = \frac{2Cr_c DF^2(z)}{DF^3(z)} \quad (49b)$$

The constant C is determined from the condition that at $z=0$, $DF(Z)=R_c$ and $u_z=V_o$

$$C = V_o \frac{R_c^2}{2} \quad (50)$$

The velocity field is, therefore, written as,

$$u_z = \frac{V_o R_c^2}{2(R_c - z \tan(\alpha + \lambda))} \quad (51a)$$

$$u_r = \frac{V_o R_c^2 r_c \tan(\alpha + \lambda)}{(R_c - z \tan(\alpha + \lambda))^3} \quad (51b)$$

$$u_\theta = 0 \quad (51c)$$

The detailed analysis and computed results for the above case will be presented in a future paper.

6. CONCLUSIONS

Some new upper bound solutions for plane strain compression and extrusion operations are presented using the ‘‘Generalized upper bound’’ technique. The interface friction behaviour is assumed to be governed by Coulombs law ($\tau = \mu p$). For compression and extrusion the velocity fields are formulated by modifying some existing ones, so as to be compatible with the interface coulomb friction condition. This implies that for extrusion through a die of wedge angle ‘ α ’, the velocity field should be that for a frictionless die of wedge angle $(\alpha + \lambda)$ ($\tan \lambda = \mu$). It is seen that the geometrical changes in the billet under continued compression are insensitive to the value of μ . Also, the effect of friction becomes significant only at higher reductions.

For die angles $\alpha=15$ and 30 degrees the present analysis yields lower upper bounds at lower ($<20\%$) and higher ($>50\%$) reductions. For $\alpha = 45$ degrees the velocity fields derived using rigid triangular elements yield lower upper bounds at all reductions and friction conditions. The results compare very well with the same obtained from finite element simulation and from experiment.

The upper bounds computed assuming radial flow are found to be equal to those obtained from velocity fields derived from the present stream function. Loads calculated assuming uniform pressure distribution at the interfaces give acceptable results only at very low values of μ ($\mu \leq 0.1$).

NOMENCLATURE

J^* = Total energy dissipation

A = a constant

D = Strip width in forging

H = Forging strip thickness, billet thickness at die entry in extrusion

Hc = Billet height at entry to die AC (Fig. 3)

L = Extrusion die length

N = Extrusion die pressure

P = Forging, extrusion punch load

p = Mean forging, extrusion pressure
 Q = Friction constant
 T = Resultant tool die traction
 V_o = Platen velocity in forging, billet velocity at entry to the extrusion die
 V_f = Product velocity in extrusion
 W_i = Internal power of deformation
 W_f = Friction power
 W_{en} & W_{ex} = Power due to velocity discontinuities at the entry and exit in the extrusion die respectively
 X, Y, X_f, Y_f = Cartesian coordinates
 v = Velocity in the direction of T
 h = Extrusion billet height at exit
 v_x, v_y = Velocity along coordinate directions
 α = Extrusion die angle
 μ = Coefficient of friction
 λ = Friction angle
 ψ = Stream function, angular coordinate of a point in radial flow.
 θ = Angular coordinate of any point on AB with respect to origin (Fig. 4a)
 r = Radial coordinate
 $\epsilon_x, \epsilon_y, \epsilon_z$ = Eulerian longitudinal strains
 $\gamma_{xy}, \gamma_{yz}, \gamma_{zx}$ = Eulerian shear strains
 $\bar{\epsilon}$ = Effective strain
 β = Bulge parameter
 σ_0 = Yield stress in compression of work material
 k = Yield stress in shear of work material
 r, θ, z = Cylindrical polar coordinates

REFERENCES

[1] W. Prager and P.G.Hodge, Theory of perfectly plastic solids .Chaman and Hall, Ltd, London(1951)

[2] D.C.Drucker, W. Prager and H.J.Greenberg. Extended limit design theorems for continuous media Of Applied mathematics, Vol p.381(1952). <http://www.jstor.org/stable/43633923>

[3] R.Hill On the state of stress in a plastic-Rigid at the yield point. Philosophical magazine ,Vol 42 868.(1951). DOI: <https://doi.org/10.1080/14786445108561315>

[4] A.P Green .The compression of ductile material between smooth dies.Philosophical magazine ,vol.42-900.(1951). DOI: 10.1080/14786445108561319

[5] W.Johnson Estimation of upper bound loads for extrusion and coining operations.proc,institution of mech,engg,173.61,(1959). https://doi.org/10.1243%2FPIIME_PROC_1959_173_017_02

[6] H.Kudo,Some analytical and experimental studies of axisymmetric cold forging and extrusion part-1.int.J.Mech.sci.2,102,(1960). DOI:10.1016/0020-7403(60)990016-3

[7] H.Kudo.Some analytical and experimental studies of axisymmetric cold forging and extrusion ,part1,Int. J.Mech.Sci.3,91,(1961). [https://doi.org/10.1016/0020-7403\(61\)90041-8](https://doi.org/10.1016/0020-7403(61)90041-8)

[8] S.Kobayashi Upper bound solutions of axisymmetric forging Problems part-1 and part-ii,Trans ASME,SERB,86,4,326(1965). <https://doi.org/10.1115/1.3428053>

[9] B.Avitzur ,Analysis of wire drawing and extrusion through conical dies of large cone angles.Trans ASME,SERB 86,4,305,91964). <https://doi.org/10.1115/1.3670543>

[10] B.Avitzur ,Flow characteristics through conical converging dies,Trans ASME,SERB,88,4,410,(1966). <https://doi.org/10.1115/1.3672673>

[11] V.Nagpal. General kinematically admissible velocity fields for some axisymmetric metal forming problems ,Trans ASME,J,Engg,Ind,96,1197(1974). <https://doi.org/10.1115/1.3438495>

[12] V.Nagpal and T.attan, Analysis of three dimensional metal flow in extrusion of shapes with the use of dual stream functions ,proc.3rd.North American metal research conf. Carnegie-Mellon university,(1975)

[13] D.Y.Yang,M.U.Kim and E.H.Lee. An analysis for extrusion of helical shapes from round billets, int.J.Mech.Sci.20,695 (1978). [https://doi.org/10.1016/0020-7403\(78\)90056-5](https://doi.org/10.1016/0020-7403(78)90056-5)

[14] D.Y.Yang and C.H.Lee, Analysis of three dimensional extrusion of sections through curved dies by conformal transformation, int.JMech ,Sci 20,541-(1978)

[15] L.C.Stepanskii, The boundaries of the areas of plastic deformation in extrusion .Russian Engg,J.(Eng translation) 43,9,40,(1963)

[16] Kozo Osakada and Yuji Niimi ,A Study on radial flow for extrusion through conical dies.Int.J.Mech.Sci,17,241,(1975). [https://doi.org/10.1016/0020-7403\(75\)90006-5](https://doi.org/10.1016/0020-7403(75)90006-5)

[17] Wei-Ching Yeh and Yeon-Sheng Yang, A Variational upper bound method for plane strain problems.J.Manu sci.Engg,118,301, (1996). <https://doi.org/10.1115/1.2831029>

[18] N.Alexandrova,Analytical treatment of tube drawing with a mandrel.Proc.int. Mech .Engg,part c 215,581 (2001). <https://doi.org/10.1243%2F0954406011520968>

[19] W.Johnson and P.B.Mellor, Engineering plasticity. Van Nostrand reinhold,London(1973)

- [20] B. Avitzur, Metal forming processes and Analysis McGraw Hill, New York (1968)
- [21] D.C. Drucker. Coulomb friction, plasticity and limit loads. Trans ASME, J. Appl Mech. 21, 71, (1954).
<https://apps.dtic.mil/dtic/tr/fulltext/u2/002902.pdf>
- [22] S. Solhjo. A note on "Barrel compression Test": A method for evaluation of friction, comput. Mater. Sci, 49, 435, (2010).
<https://doi.org/10.1016/j.commatsci.2010.04.047>
- [23] G.W. Rowe. Principles of metal working. Edward Arnold, London. (1968)
- [24] D. Westwood and J.F. Wallace, Upper bound values for the loads on a rigid plastic body in plane strain J. Mech. Engg sci, 2, 179 (1960).
https://doi.org/10.1243%2FJMES_JOUR_1960_002_027_02
- [25] J.W. Green and J.F. Wallace. Estimation of load and torque in the hot rolling process S. J. Mech. Engg Sci, 4, 136, (1962).
https://doi.org/10.1243%2FJMES_JOUR_1962_004_020_02
- [26] J.W. Green, L.G.M. Sparling and J.F. Wallace. Shear plane theories of hot and cold rolling. J. Mech. Engg sci, 6, 219, (1964).
https://doi.org/10.1243%2FJMES_JOUR_1964_006_033_02
- [27] H. Ernst and M.E. Merchant. Chip formation, friction and high quality machined surfaces. Trans A.S.M., 29, 299. (1941)
- [28] P. Oxley. Allowing for friction in estimating upper bound loads. Int. J. Mech, sci, 5, 183, (1963)
- [29] E.M. Rubio, C. Gonzalez, M. Marcos and M.A. Sebastian. Energetic analysis of tube drawing processes with fixed plug by upper bound method. J. Mater. proc Technol, 177, 175 (2006).
<https://doi.org/10.1016/j.jmatprotec.2006.03.193>
- [30] I.F. Collins. The upper bound theorem for rigid/plastic solids generalized to include coulomb friction. J. Mech. phy solids. 17, 323, (1969).
[https://doi.org/10.1016/0022-5096\(69\)90021-0](https://doi.org/10.1016/0022-5096(69)90021-0)
- [31] H.S. Yu and S.W. Sloan. Upper bound limit analysis of a rigid plastic body with frictional interfaces. Int. J. mech. sci. 36, 219, (1994).
[https://doi.org/10.1016/0020-7403\(94\)90071-X](https://doi.org/10.1016/0020-7403(94)90071-X)
- [32] C.H. Lee and T. Atan. Influence of flow stress and friction upon metal flow in upset forging of rings and cylinders, Trans A.S.M.E. J. Engg, ind. 94, 775 (1972).
<https://doi.org/10.1115/1.3428250>
- [33] W.H. Press, S.A. Teukolsky, W.T. Vetterling and B.P. Flannery. FORTRAN, numerical recipes, Cambridge university press. 1986.
- [34] X.G. Fan, Y.D. Dong, H. Yang, P.F. Gao and M. Jhan. Friction assessment in uniaxial compression test - A new evaluation method based on local bulge profile. J. Matl. proc. Technology 243, 282 (2017).
<https://doi.org/10.1016/j.jmatprotec.2016.12.023>
- [35] W. Johnson, Extrusion through wedge-shaped dies part-1. Journal of the mechanics and physics of solids, 3, 218, 1955. DOI: 10.1016/0022-5096(55)90014-4
- [36] W. Johnson. Extrusion through wedge-shaped dies part-ii. Journal of mechanics and physics of solids, 224. 1955. [https://doi.org/10.1016/0022-5096\(55\)90015-6](https://doi.org/10.1016/0022-5096(55)90015-6)
- [37] N.S. Das. A Class of slip line field, solutions for compression and extrusion with slipping friction. Ph.d thesis. Submitted to sambalpur university 1983. <http://hdl.handle.net/10603/187839>
- [38] W. Johnson Experiments in plane strain extrusion Journal of the mechanics and physics of solids. 4, 269 (1956). [https://doi.org/10.1016/0022-5096\(56\)90036-9](https://doi.org/10.1016/0022-5096(56)90036-9)